

Asymmetry induces Q-band split in the electronic excitations of magnesium porphyrin

Xiankai Jiang, Yi Gao, Ratnesh Lal, Jun Hu & Bo Song

To cite this article: Xiankai Jiang, Yi Gao, Ratnesh Lal, Jun Hu & Bo Song (2018): Asymmetry induces Q-band split in the electronic excitations of magnesium porphyrin, *Molecular Physics*, DOI: [10.1080/00268976.2018.1444207](https://doi.org/10.1080/00268976.2018.1444207)

To link to this article: <https://doi.org/10.1080/00268976.2018.1444207>

 [View supplementary material](#) 

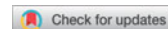
 Published online: 12 Mar 2018.

 [Submit your article to this journal](#) 

 [View related articles](#) 

 [View Crossmark data](#) 

RESEARCH ARTICLE



Asymmetry induces Q-band split in the electronic excitations of magnesium porphyrin

Xiankai Jiang^a, Yi Gao^{b,c}, Ratnesh Lal^d, Jun Hu^{b,c} and Bo Song^a

^aTerahertz Technology Innovation Research Institute, Shanghai Key Laboratory of Modern Optical System, Terahertz Science Cooperative Innovation Center, School of Optical-Electrical Computer Engineering, University of Shanghai for Science and Technology, Shanghai, China;

^bKey Laboratory of Interfacial Physics and Technology at Shanghai Institute of Applied Physics, Chinese Academy of Sciences, Shanghai, China;

^cDivision of Water Science and Technology, Shanghai Institute of Applied Physics, Chinese Academy of Sciences, Shanghai, China; ^dDepartment of Bioengineering, Nano-bio-imaging and Devices Laboratory, University of California San Diego, La Jolla, CA, USA

ABSTRACT

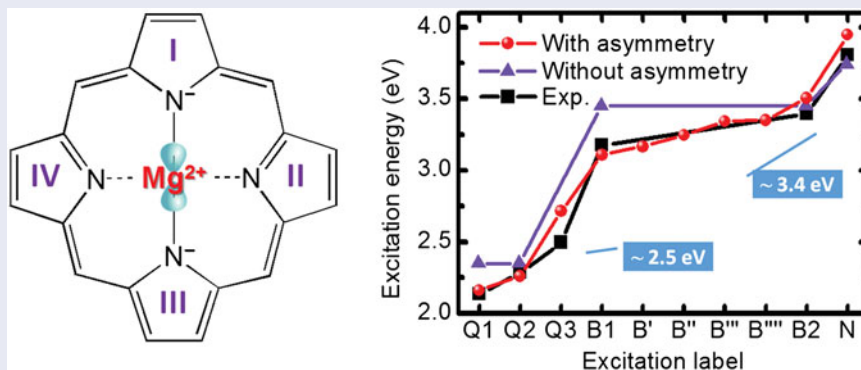
The electronic excitations of magnesium porphyrin (MgP), a molecular model for understanding the physics in light harvesting by biological systems, have been studied extensively. However, the theoretical underpinning of experimental measurements is still lacking, especially about the sub-bands in absorption spectrum. Here we propose that an asymmetry of MgP based on the uneven charge distribution of pyrrole rings and the linear structure of sp hybridised orbitals in Mg can largely influence the electronic excitations. Upon a very weak asymmetry of Mg-pyrrole bindings in MgP being introduced through the uneven distribution of charge, three different excitations are observed in the Q-band region of the experimental spectrum. Additionally, the predicted B-band excitations are highly correlated (10^{-2} eV level) with experimental measurements. In contrast, without this asymmetry, there are only two degenerate excitations in the Q-band region, and low agreement (10^{-1} eV level) of the B-band excitations with the experiment. The key physics of the unexpected and observable asymmetry in MgP is the ability of Mg to form sp hybridised orbitals on the third shell upon Mg binding to the nitrogen of pyrrole ring. Our findings provide new insight for high-energy efficiency of natural as well as artificial light-harvesting system for energy challenge.

ARTICLE HISTORY

Received 30 September 2017
Accepted 12 February 2018

KEYWORDS

Electronic excitation;
magnesium-porphyrin
asymmetry; photosynthetic
light-harvesting



1. Introduction

Our understanding of the high-efficiency energy transfer in photosynthesis is essentially important for designing light-harvesting devices as a solution for the energy challenge [1–10]. Magnesium porphyrin (MgP) has traditionally been used as a molecular model to obtain fundamental characteristics of the electronic excitation in the photosynthetic light-harvesting process [11]. In 1959,

Gouterman [12] first predicted the Q-band at approximately 2 eV for MgP due to the D_{4h} symmetry of its molecular conformation, which was confirmed by *ab initio* calculations [11,13–20]. One excitation (or two degenerate excitations), corresponding to the Q-band of MgP, was found at 2.15 eV by calculations based on the multiconfiguration second-order perturbation theory (CAS-PT2) [17], 1.68 eV by symmetry-adapted-

CONTACT Bo Song  bsong@usst.edu.cn

 Supplemental data for this article can be accessed at  <https://doi.org/10.1080/00268976.2018.1444207>.

© 2018 Informa UK Limited, trading as Taylor & Francis Group

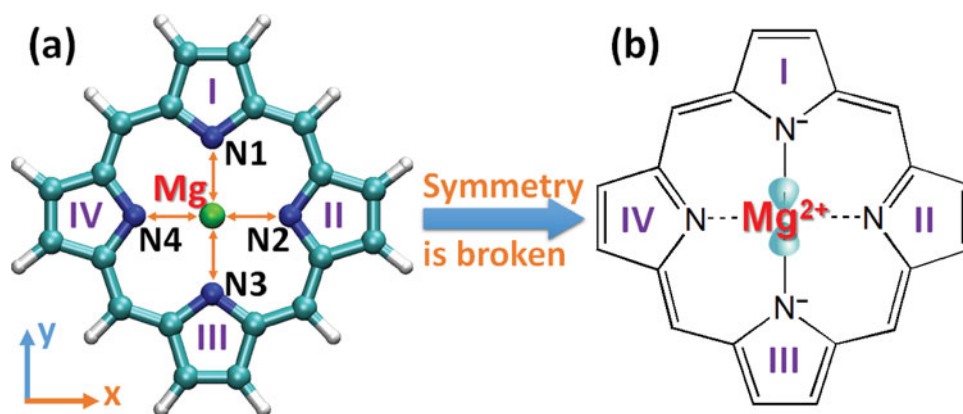


Figure 1. Schematic representation of asymmetry in MgP triggered by the orbital hybridisation of Mg ion. (a) A D_{4h} symmetric MgP molecule with an identical distance of Mg to the N1, N2, N3 and N4 of the pyrrole rings I–IV. Besides the spheres labeled by Mg and N, the rest of spheres denote the C and H atoms by the large and small, respectively. (b) Asymmetry caused by the orbital hybridisation of Mg^{2+} and the subsequently different interactions with the pyrrole rings. The dumbbell-shaped clouds indicate the hybridised orbitals potentially in the Mg ion. The interactions (solid lines) of Mg^{2+} with the N^- in the pyrrole rings I and III may be relatively stronger than those (dashed lines) with the N in the pyrrole rings II and IV, which is potentially triggered by the asymmetric structure of hybridised orbitals (dumbbell-shaped clouds) in the Mg ion.

cluster configuration-interaction calculations (SAC-CI) [17], 2.52 eV by configuration interaction with single excitation calculations (CIS) [18] and 2.47 eV by calculations based on the time-dependent density functional theory (TDDFT) [18]. Significantly though, the theoretical calculations are still not consistent with experimental results. For example, two Q sub-bands as well as one shoulder peak at their high-energy side were experimentally observed clearly for Mg etioporphyrin I (MgEtioP) [21], a molecule regarded with the identical electronic spectrum of MgP in the ultraviolet–visible light region [20], and three electronic transitions were identified in the Q-band region of chlorophyll *a* spectrum by linear dichroism [22]. It is hard to explain the above band splitting based on the previous calculations. Very few works employed vibronic coupling effects to solve this problem, but only two electronic excitations were achieved responsible for the Q-band [23,24]. Moreover, the quantitative difference of the B-band with the experimental data is large, ~ 0.2 eV for CAS-PT2 calculations [11,17], ~ 0.1 eV for SAC-CI [17] and ~ 1.5 eV for CIS [18]. Additionally, in the TDDFT calculations of MgP, the excitations depended on the applied basis set and functional [18–20], which leads to difficulty in the estimation and application of the results. All of these inconsistencies have seriously hindered our deeper understanding of the quantum mechanism underlying the energy transfer in light harvesting.

From the physical point of the view, a non-split Q-band in light absorption spectrum should be a result of MgP D_{4h} symmetry, which has been strictly derived based on the four-orbital model [12]. MgP was usually regarded with a D_{4h} symmetry according to the

molecular conformation (Figure 1(a)). With the experiments and theoretical calculations of molecular conformation and vibrations, this symmetry assumption has been widely accepted [25]. However, the split of Q-band in the light absorption spectrum [21] implied that the above symmetry might be broken in MgP. Recent high-accuracy *ab initio* calculations of coupled cluster with single and double and perturbative triple excitations (CCSD(T)) showed that the s and p orbitals of Mg were able to be hybridised upon binding to other atoms, implying a symmetry reduction of Mg p orbitals [26]. Additionally, by terahertz spectroscopy, significant covalent character was found in Mg–H binding, although the electronegativity was 1.31 for Mg and 2.20 for H [27]. Moreover, very recent CCSD(T) studies reported that a Q-band split occurred in a D_{4h} symmetric iron-porphyrin (its molecular conformation and absorption spectrum very similar to MgP), which implies the existence of D_{2h} electronic excitation in a D_{4h} molecule [28]. Therefore, similar symmetry-breaking must potentially happen when Mg^{2+} interacts with pyrrole rings in MgP, leading to a difference in the bindings of Mg^{2+} with the pyrrole rings along the up–down and left–right directions (Figure 1(b)). These would further induce some asymmetry in MgP properties, especially in its electronic excitations.

The asymmetry in MgP is very weak, which will be easily neglected by conventional *ab initio* calculations with the applied approximations in the methods [11,13–20]. Fortunately, the calculation and analysis based on functional fragments have been successfully developed and applied in the studies of sensitive properties in bio-molecules, where weak inter- or

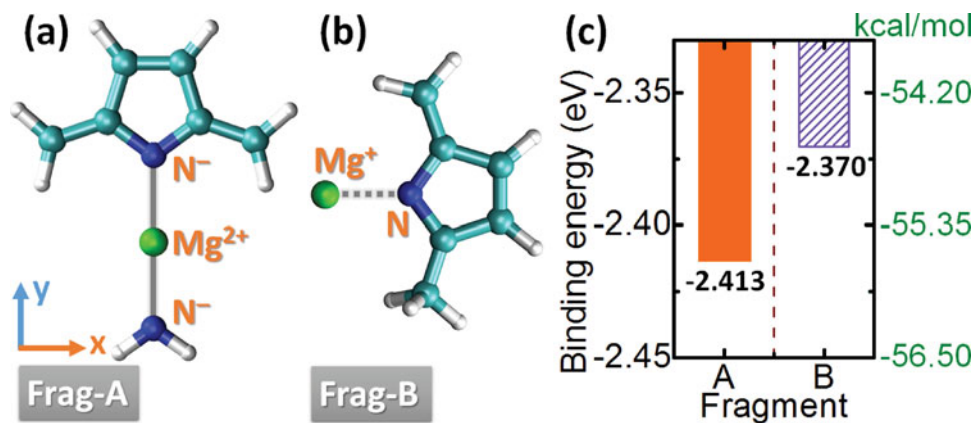


Figure 2. Pyrrole ring-based fragments for retaining MgP asymmetry. (a) and (b) Fragments partitioned from MgP molecule. Besides the spheres labeled by Mg²⁺, N⁻ and N, the rest of spheres denote the C and H atoms by the large and small, respectively. The solid (between Mg²⁺ and N⁻) line and dashed line (between Mg²⁺ and N) represent the relatively stronger (a) and weaker (b) bindings of Mg with N, respectively. (a) Fragment A (Frag-A) consisting of the pyrrole ring I (or III) (see Figure 1(b)). Mg²⁺ ion simultaneously binds to the N⁻ of the pyrrole ring and [NH₂]⁻ group, causing the reduction of Mg²⁺ to Mg⁺. (b) Fragment B (Frag-B) consisting of the pyrrole ring II (or IV). Mg⁺ ion binds to the N atom of the pyrrole ring. (c) Binding energies of Mg with the pyrrole rings of Frag-A and Frag-B. The difference between them is only 0.043 eV (0.99 kcal/mol), very close to the thermal fluctuation (~ 0.03 eV = 0.69 kcal/mol) at a room temperature.

intra-molecular interactions usually play an important role in modulating the behaviours of complicated molecules [29,30]. We believe that this approach can be used in the situation of MgP light excitations.

Here, we first partitioned the molecule into two types of isolated pyrrole-ring involved fragments: (a) Mg relatively stronger binding to a pyrrole ring (Figure 2(a)), and (b) Mg relatively weaker binding to a pyrrole ring (Figure 2(b)). The asymmetry of MgP, caused by the difference of Mg-pyrrole bindings, thus can be retained in the different electronic excitations of these fragments. Based on a model Hamiltonian of MgP molecule built and parameterised from the *ab initio* results of the fragments, we calculated the excitation energies of the molecule and found three electronic excitations corresponding well to the two sub-bands and one shoulder peak of the Q-band, respectively. For the excitations belonging to the B-band of MgP absorption spectrum, our calculations reached a level of 10^{-2} eV accuracy as compared to the experiments. Finally, we revealed that the asymmetry of MgP was triggered by the linear structure of sp hybridised orbitals on the third shell of Mg ion.

2. Methods

Ab initio calculations: Our *ab initio* calculations were based on the density functional theory (DFT) and the TDDFT, as implemented in the Gaussian09 package [31], within the generalised gradient approximation (GGA). We used Becke's three-parameter hybrid exchange functional with Lee–Yang–Parr gradient-corrected correlation (B3LYP) [32]. A basis set 6-31+G(d,p), as

augmented by both the polarisation and diffuse functions [33], was applied for all atoms. The geometry optimisations of all compounds were carried out by DFT with the Bery algorithm [34]. The optimised stationary points were identified as minima or first-order saddle points. Electronic excitations were calculated by TDDFT.

3. Results and discussions

3.1. Pyrrole-ring based fragments for retaining MgP asymmetry

The key approach in our study was to retain the asymmetry of MgP during the calculations. We first partitioned the molecule into several pyrrole-ring involved fragments. The geometry optimisation was performed on MgP molecule by the calculations based on the DFT, and a symmetric conformation was obtained with an identical distance 2.066 Å of Mg to the N1, N2, N3 and N4 atoms of the pyrrole rings I–IV (Figure 1(a)). Fixing the bond lengths and angles, according to the asymmetric characteristics of Mg-pyrrole bindings shown in Figure 1(b), we then partitioned the molecule into two types of isolated fragments (Figure 2(a,b)): the fragment A (denoted as Frag-A) consisting of the pyrrole ring I (or III), and the fragment B (denoted as Frag-B) consisting of the pyrrole ring II (or IV). For Frag-A, the N atom, initially in the pyrrole ring III (or I) opposite to the remained pyrrole I (or III), was kept and then passivated by two H atoms to form a [NH₂]⁻ group (Figure 2(a)). The C atoms linked to the left and right sides of the pyrrole ring were passivated by two H atoms, respectively. In this way, a dangling

bond appeared in the N atoms of the pyrrole ring and $[\text{NH}_2]^-$ group, which promised the formed Mg-pyrrole binding like that of Mg with the pyrrole ring I (or III) in MgP (Figure 1(b)). Further analysis of the fragment showed that the Mg ion had a Mulliken charge [35] of $+0.8 e$, indicating that the Mg^{2+} is reduced upon binding to the two N atoms of the fragment. Therefore, we applied an Mg^+ ion for Frag-B (Figure 2(b)). The two carbon atoms linked to the pyrrole ring of this fragment were then passivated by two and three hydrogen atoms, respectively, which promised no dangling bond in the N atom of Frag-B, and subsequently the Mg-pyrrole binding like that of Mg with the pyrrole ring II (or IV) in MgP (Figure 1(b)). We have also compared the strengths of Mg binding to the pyrrole rings of the fragments. Considering the Mg–N bond order was 0.34 in Frag-A and 0.07 in Frag-B, we applied the following equation to calculate the binding energies of Mg,

$$E_{\text{binding}}^{\text{Frag-A}}(\text{Mg}) = E(\text{Frag} - \text{A}) - E(\text{Pyr} - \text{A}) - E(\text{MgNH}_2), \quad (1)$$

$$E_{\text{binding}}^{\text{Frag-B}}(\text{Mg}) = E(\text{Frag-B}^+) - E(\text{Pyr} - \text{B}) - E(\text{Mg}^+), \quad (2)$$

where $E_{\text{binding}}^{\text{Frag-A}}(\text{Mg})$ and $E_{\text{binding}}^{\text{Frag-B}}(\text{Mg})$ denote the binding energies of Mg with the pyrrole rings of Frag-A and Frag-B, respectively. The labels Pyr-A and Pyr-B represent Frag-A without the MgNH_2 group and Frag-B without Mg^+ , respectively. In Equation (1), $E(\text{Frag-A})$, $E(\text{Pyr-A})$ and $E(\text{MgNH}_2)$ indicate the energies of Frag-A, Pyr-A and the MgNH_2 group, respectively. In Equation (2), $E(\text{Frag-B}^+)$, $E(\text{Pyr-B})$ and $E(\text{Mg}^+)$ mean the energies of the positively-charged Frag-B, the Pyr-B and the Mg^+ ion, respectively. As shown in Figure 2(c), the binding energy of Mg with the pyrrole ring was -2.413 eV for Frag-A and -2.370 eV for Frag-B, indicating that the binding strength of Mg in Frag-A is a little stronger than that in Frag-B. Their difference was only 0.043 eV (0.99 kcal/mol), much weaker than the Mg-pyrrole interactions and a little larger than the thermal fluctuation (~ 0.03 eV = 0.69 kcal/mol) at a room temperature. Therefore, the weak asymmetry in MgP could be retained through Frag-A and Frag-B with the help of the weak difference in the Mg-pyrrole bindings on a sub-picosecond scale.

3.2. Different electronic excitations of the fragments induced by MgP asymmetry

To explore the influence of the Mg-pyrrole binding asymmetry on the electronic excitations, we calculated the single-electron excitation energies of Frag-A and

Table 1. Comparison in the energies (eV) of the optically allowed excitations between the fragments A and B.

TDDFT		Experiment ^a	
Frag-A	Frag-B	MgEtioP	Assignment
2.219	–	2.14, 2.29 ($\sim 2.5^b$)	Q
3.268	3.243	3.18 ($\sim 3.4^c$)	B
3.380	3.348	–	

^a Gas-phase absorption spectrum of MgEtioP²¹.

^b A shoulder peak at the high-energy side of the Q-band.

^c A shoulder peak at the high-energy side of the B-band.

Frag-B based on the TDDFT. The results are shown in Table 1. In the region close to the Q-band of MgP absorption spectrum, there was an excitation energy of 2.219 eV from Frag-A and no excitation observed from Frag-B with a non-vanishing value of oscillator strength. In the region close to the B-band, there were two excitation energies (3.268 eV, 3.380 eV) for Frag-A and two excitation energies (3.243 eV, 3.348 eV) for Frag-B, which were related to the major peak (3.18 eV) and the shoulder peak (~ 3.4 eV) of the MgEtioP B-band. These results indicate that the asymmetry of MgP can be clearly presented in the difference of electronic excitations between Frag-A and Frag-B, especially the excitation related to the Q-band. Therefore, although the effect of MgP asymmetry may be very weak and ignorable in the Mg-pyrrole interactions (Figure 2(c)) and subsequently molecular conformation (Figure 1(a)), it would significantly affect the electronic excitations of MgP.

3.3. Effects of the asymmetry on the structure in electronic excitations of MgP

Because the coupling was weak between the pyrrole rings of MgP (see the details in Supplementary Information), we could introduce a model consisting of four quantum dots (QDs) (I, II, III and IV) (Figure 3(a)) to calculate the excitation energies of MgP. Based on the excitation energies of Frag-A and Frag-B (Table 1) and the coupling strengths of pyrrole rings from the *ab initio* calculations on double-pyrrole-ring involved fragments (Figures S1 and S2 in Supplementary Information), a Hamiltonian was built for the model with three occupied levels for QDs I and III (Figure 3(b)) and two occupied levels for QDs II and IV (Figure 3(c)),

$$H = \sum_{m=\text{I,III}} \left[\varepsilon_m^q a_{m,q}^+ a_{m,q} + \sum_i \varepsilon_{m,i}^b a_{m,i}^+ a_{m,i,b} \right] + \sum_{m=\text{II,IV};i} \varepsilon_{m,i}^b a_{m,i}^+ a_{m,i,b}$$

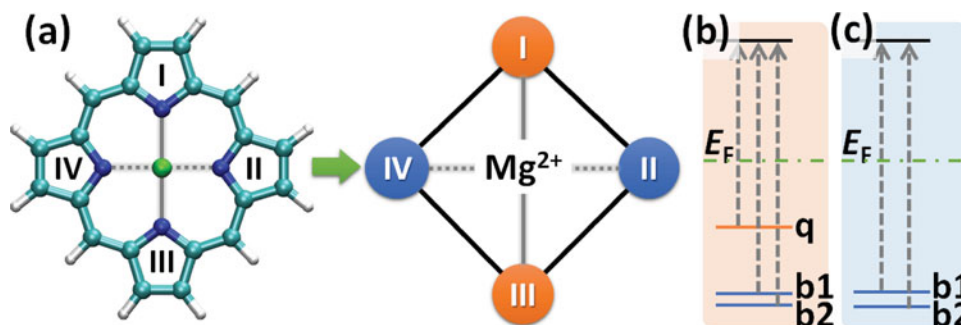


Figure 3. An asymmetric model for MgP molecule based on the *ab initio* calculations of fragments. (a) A model consisting of four quantum dots (QDs) (I, II, III and IV) that correspond to the four pyrrole rings (I, II, III and IV) of MgP. (b) and (c) The level structures of QDs related to the Q and B bands of MgP absorption spectrum. The dot-dashed line denotes the Fermi level. The labels q, b1 and b2 indicate the levels related to the Q- and B-band excitations, respectively. (b) The level structure for QDs I and III. (c) The level structure for QDs II and IV.

$$\begin{aligned}
 & + \sum_{m \neq n} t_{m,n}^q \left(a_{m,q}^+ a_{n,q} + a_{n,q}^+ a_{m,q} \right) \\
 & + \sum_{m \neq n; i, j} t_{m,n; i, j}^b \left(a_{m,i,b}^+ a_{n,j,b} + a_{n,j,b}^+ a_{m,i,b} \right),
 \end{aligned}$$

where $m, n = I, II, III$ and IV . Due to no excitation of Frag-B with a non-vanishing oscillator strength related to the Q-band of MgP spectrum (see Table 1), only the levels responsible for the B-band were introduced in QDs II and IV. The label ε_m^q represents the energy of the occupied level in the QD m related to the Q-band of MgP light absorption spectrum, while $\varepsilon_{m,i}^b$ denotes the energies of the two levels ($i = 1$ or 2) related to the B-band. $a_{m,q}^+$ ($a_{m,q}$) and $a_{m,i,b}^+$ ($a_{m,i,b}$) denote the creation (annihilation) operators for the electron at the (m, q) and (m, i, b) levels, respectively. The parameter $t_{m,n}^q$ stands for the coupling strength between the (m, q) and (n, q) levels, and $t_{m,n; i, j}^b$ for that between the (m, i, b) and (n, j, b) levels, where $m \neq n$. Considering that the difference of excitations in the Q, B and N bands of MgP mainly depended on the

states under the Fermi level [14,15], we took the energy of electron in the excited state as the reference. Therefore, based on the excitation energies of Frag-A and Frag-B, we calculated the energies of occupied levels as follows: $\varepsilon_1^q = \varepsilon_{III}^q = -2.219$ eV, $\varepsilon_{1,1}^b = \varepsilon_{III,1}^b = -3.268$ eV, $\varepsilon_{1,2}^b = \varepsilon_{III,2}^b = -3.380$ eV, $\varepsilon_{II,1}^b = \varepsilon_{IV,1}^b = -3.243$ eV, $\varepsilon_{II,2}^b = \varepsilon_{IV,2}^b = -3.348$ eV. From the calculations of double-pyrrole-ring involved fragments (see Figures S1 and S2 in Supplementary Information), the coupling parameters between QDs were obtained as the following. For the nearest neighbouring QDs, $t_{m,n; i, j}^b = 0.2$ eV upon $i = j$, and 0.1 eV upon $i \neq j$, while $t_{m,n}^q$ was vanishing due to no corresponding levels applied in QDs II and IV. For the next neighbouring QDs I and III, $t_{m,n; i, j}^b = 0.05$ eV upon $i = j$, and 0.02 eV upon $i \neq j$, while $t_{m,n}^q = 0.05$ eV. The coupling of QDs II and IV was ignored because the bindings of Mg with the pyrrole rings II and IV was weaker than those with the pyrrole rings I and III. The single-electron excitation energies of the four-QD model were then calculated based on this Hamiltonian. The results are shown in Figure 4(a).

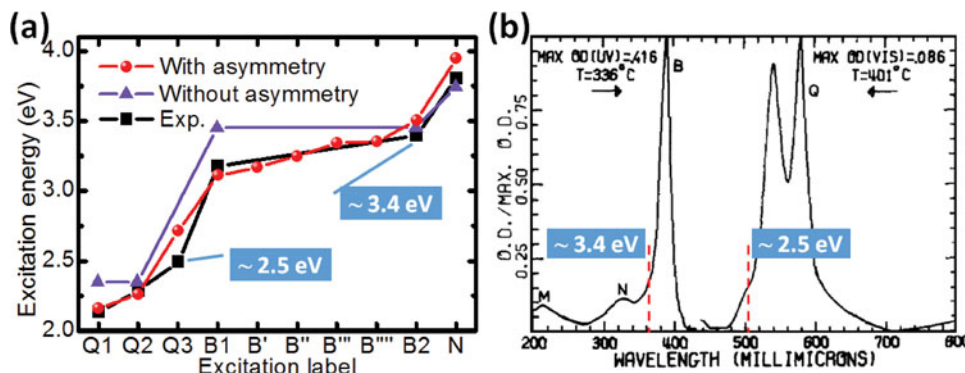


Figure 4. Electronic excitations of MgP. (a) Effects of the asymmetry on the electronic excitations of MgP. The spheres and triangles indicate the calculated excitation energies with and without the asymmetry of Mg-pyrrole bindings, respectively, while the squares denote the experimental data [21]. (b) Gas-phase absorption spectrum of MgEtioP [21]. The vertical dashed lines indicate the locations of shoulder peaks. Besides the major peaks, there are two shoulder peaks at the high-energy sides of the Q-band (~ 2.5 eV) and the B-band (~ 3.4 eV), respectively. Reprinted with permission from Edwards *et al.* [21]. Copyright © 1970 Published by Elsevier Inc.

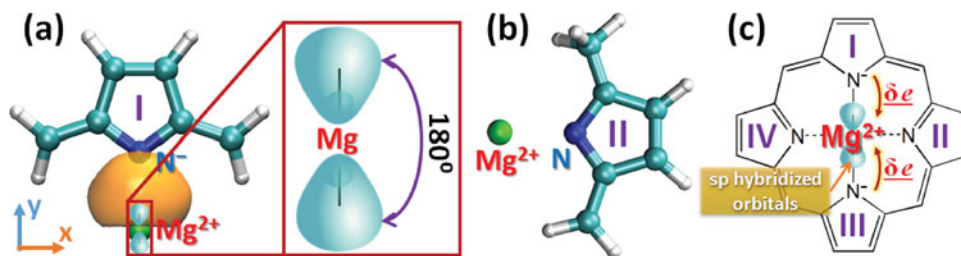


Figure 5. Origin of the asymmetry in MgP. (a) and (b) Two molecular models employed for revealing the origin of MgP asymmetry. Besides the spheres labeled by Mg^{2+} , N^- and N , the rest of spheres denote the C and H atoms by the large and small, respectively. The spindle-shaped cloud located between Mg^{2+} and N^- with the isosurface of $0.03 \text{ e}/\text{\AA}^3$ denotes the electron distribution of the Mg–N covalent orbital. The Mg–N distance remains at the identical value in MgP. (a) Model A: Mg^{2+} binding to a pyrrole ring from the pyrrole I of MgP. Upon Mg^{2+} binding to the pyrrole ring, a few electrons (0.86 e) transfer from the pyrrole to Mg^{2+} , and then majorly occupy the 3s and 3py orbitals of Mg ion. Right: The 3s orbital of Mg hybridises with the 3py orbital, leading to two sp hybridised orbitals (dumbbell-shaped clouds). Both the two front and two back lobes of the hybridised orbitals point in opposite directions, resulting in a linear structure for the transferred electrons in real space. The sp hybridised orbital further forms a covalent orbital (spindle-shaped cloud) with the orbital of the N in the pyrrole ring. (b) Model B: Mg^{2+} binding to a pyrrole ring from the pyrrole II of MgP. Very few electrons (0.21 e) transfer from the pyrrole to Mg^{2+} , and then no covalent orbital appears between the Mg and N. (c) Schematic representation for the origin of MgP asymmetry. Upon Mg^{2+} interacting with the pyrrole rings in MgP, a few electrons transfer to the Mg ion (arrowhead curves, $\delta \sim 0.5$), inducing the hybridisation of 3s and 3py orbitals in the ion. The sp hybridised orbitals (dumbbell-shaped clouds) of Mg with a linear structure then triggers the asymmetry of MgP.

Split of Q-band excitations was observed. Based on the above calculations, we successfully obtained the split excitations responsible for the Q-band. In the region less than 3.0 eV, three excitation energies (2.158 eV, 2.258 eV and 2.713 eV, red spheres in Figure 4(a)) were observed when the asymmetry of Mg–pyrrole bindings was introduced by the fragments, consistent with the split two sub-bands (2.14 eV, 2.29 eV) and one shoulder peak (~ 2.5 eV) of the Q-band in MgP absorption spectrum (Figure 4(b)). In contrast, in the results (violet triangles in Figure 4(a)) without this asymmetry (namely, TDDFT calculations directly on the symmetric MgP (Figure 1(a))), only two degenerate excitations were observed with an energy of 2.358 eV, which obviously disagreed with the experimental observations of the split Q-band. It is clear now that this inconsistency is attributed to the D_{4h} symmetry existing in MgP due to the approximations in the conventional TDDFT calculations.

High accuracy of B-band calculations was achieved. Our calculations with the asymmetry also showed a very high accuracy in the B-band excitations. For the region between 3.0 eV and 3.5 eV, when the asymmetry was introduced, there were two groups of excitation energies (3.106 eV, 3.164 eV, 3.243 eV) and (3.340 eV, 3.48 eV, 3.500 eV), which agreed with the major (3.18 eV) and shoulder (~ 3.4 eV) peaks in the experimental B-band, respectively, with a difference less than 0.1 eV. However, in the absence of the asymmetry, there were two degenerate excitations of 3.458 eV, which only matched the shoulder peak of the experimental B-band, but was far from the major peak.

Additionally, we also observed the excitation that was responsible for the N-band. In the region larger than

3.5 eV, there were values of 3.945 eV and 3.751 eV for the cases with and without the asymmetry, respectively, which corresponded to the N-band (3.81 eV) of MgP absorption spectrum.

All of these results obviously indicate that the asymmetry of Mg–pyrrole bindings play an important role in the structure of MgP electronic excitations, especially in the Q and B bands that are the functional excitations practically devoted for the light harvesting in photosynthesis.

3.4. An sp hybridisation of Mg ion as a chemical basis of MgP asymmetry

In order to further reveal the chemical basis for the unbalanced charge distribution of pyrrole rings and subsequent asymmetry in MgP (Figure 1(b)), we explored the interactions of Mg^{2+} with the pyrrole rings I and II. Two molecular models were employed as follows: an Mg^{2+} ion binding to a pyrrole ring from the pyrroles I (denoted as Model A, Figure 5(a)) and II (denoted as Model B, Figure 5(a)) of MgP, respectively. The methods similar to the previous fragment preparation were applied to prepare the models. A dangling bond thus existed on the N atom of pyrrole in Model A, not in Model B. The Mg–N distances in both models remained as the identical value in MgP. First, we compared the ability of the pyrrole ring donating electron for Mg^{2+} between the models. As shown by natural bond orbital (NBO) analyses, there were 0.86 electrons transferring from the pyrrole ring to Mg^{2+} in Model A, and only 0.21 electrons transferring in Model B, which indicated that more electrons were donated by the pyrrole ring for Mg^{2+} in Model A than in Model B. Further NBO analyses presented that the

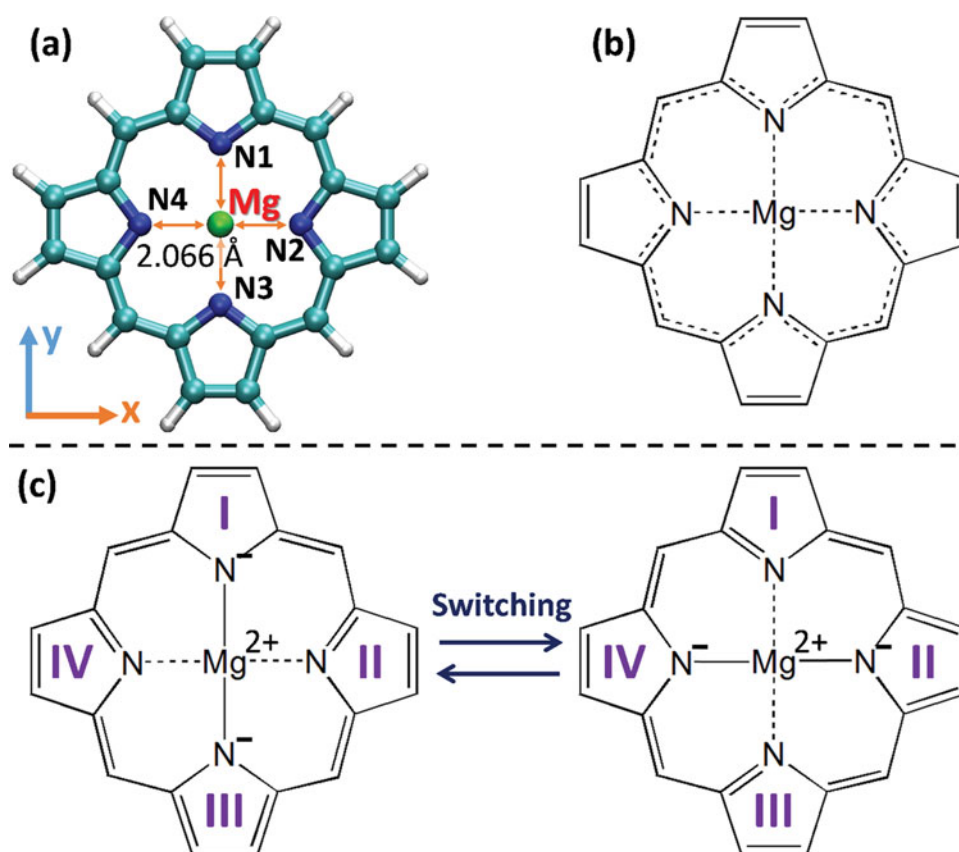


Figure 6. Two potential views for the distribution of '2-' charges in the four pyrrole rings of MgP molecule. (a) D_{4h} molecular conformation of MgP. The Mg-N distances are identical. (b) According to the D_{4h} conformation of MgP, the '2-' charges are evenly distributed to the four pyrroles. (c) According to the resonance structures of MgP, the '2-' charges are only distributed to the two of four pyrroles, and the other two are neutral. The left and right indicate two resonance structures of MgP. The solid and dashed lines denote the covalent and non-covalent bonds, respectively.

transferred electron in Model A mostly occupied the 3s and 3py orbitals of Mg ion, while these two orbitals were hybridised, resulting in two sp hybridised orbitals with an angle of 180° between them (Figure 5(a), right). It should be noted that this asymmetry of Mg ion induced by the sp hybridised orbitals would be very weak because there were few electrons ($\sim 0.5 e$) occupying these hybridised orbitals. Furthermore, an occupied covalent orbital was observed containing 20% electrons from one of the sp hybridised orbitals in Mg and 80% electrons from one of three sp^2 hybridised orbitals in N, indicating that a chemical bond forms between the Mg and N. In contrast, for Model B, the asymmetry of Mg ion induced by sp hybridisation could almost be ignored because there were only 0.21 electrons transferring to Mg^{2+} , significantly less than those (0.86 e) in Model A. Subsequently, no covalent orbital was observed between Mg and N in this model, clearly different from the situation in Model A. Additionally, we have also observed the 3s-3py hybridisation of Mg ion in Frag-A, although the hybridisation degree was less than that in Model A. All of these results suggest that

it is the sp hybridisation of orbitals in Mg ion that provides a basis of the uneven charge distribution and consequent asymmetry in MgP (further discussion in Section 3 of Supplementary Information).

3.5. Relation to MgP resonance structures

For the MgP molecule, there are two views for the distribution of '2-' charges in the four pyrrole rings: (1) according to the D_{4h} molecular conformation of MgP, the '2-' charges are evenly distributed to the four pyrroles (Figure 6(a,b)); (2) according to the resonance structures of MgP, the '2-' charges are only distributed to the two of four pyrroles and the other two are neutral (Figure 6(c)). The first view leads to the Gouterman model, which cannot directly provide the Q-band split. If the second view is applied (with the switching between two resonance structures of MgP), the split can be well understood due to the symmetry-breaking with help of our previous studies. Following the second view, at some time, the pyrroles I and III are negatively charged and the pyrroles II and IV

are neutral (the left structure of Figure 6(c)). The Mg^{2+} ion then prefers binding to the N of pyrroles I and III because the negative charges are majorly localised at N. Some electron of the negatively-charged N will transfer to the Mg^{2+} ion due to that the 3s and 3p orbital of Mg^{2+} ion is empty. The transferred electron further causes a sp hybridisation on Mg ion along the y direction, which induces a formation of covalent orbital with the nitrogen (N1 and N3). A similar case (the right structure of Figure 6(c)) can also happen at other time due to the resonance structure switching.

The key is the lifetime of the state, i.e. the time scale of the switching between two resonance structures. The times of electron excitation and tunnelling have been reported to be on a femtosecond scale (<10 fs) [36–39], and thus the nuclear movement can be estimated on a picosecond scale because the mass ratio of nucleus to electron is on a scale of $10^3:1$ for the atoms in MgP. The existence of sp hybridised orbital of Mg and subsequent Mg–N covalent bonds would slow down the electron transfer between pyrrole rings, and then result in the switching of two resonance structures reaching an interval between the two time scales above. (More discussions of the time-scale estimations above are shown in Section 3 of Supplementary Information.) One of the resonance structures is thus observed by the absorption spectra (fs scale), which presents a property of D_{2h} symmetry, but not D_{4h} .

4. Conclusion

In summary, we showed that the calculations based on the asymmetry assumption of MgP provides a much better result on the structure of the electronic excitations than the conventional calculations based on the symmetry assumption. For the excitations responsible to the B-band of MgP absorption spectrum, when the asymmetry was introduced, the calculations could reach a level of 10^{-2} eV accuracy as compared with the experiments. More importantly, three excitations were observed corresponding to the Q-band, consistent with the experimental spectrum. All of these observations were attributed to the fact that the D_{4h} symmetry was broken by the different interactions of Mg with the pyrrole rings, which benefitted from the linear structure of sp hybridised orbitals on the third shell of Mg after a few electrons transferring from the negatively-charged pyrrole rings to Mg^{2+} . Our findings will shed a new insight on the understanding of the quantum mechanism of the high-energy efficiency in light-harvesting system, promote the studies on the quantum effects in biological systems, and inspire new ideas for the materials and device designing of artificial photosynthesis.

Acknowledgments

We gratefully acknowledge professors Anthony J. Leggett, Ping Ao, Xiaomei Zhu and Hong Jiang for their helpful discussions.

Disclosure statement

The authors declare no conflict of interest.

Funding

Key Research of CAS [grant number KJZD-EW-M03]; National Natural Science Foundation of China [grant number 11290164]; Open Funding Project of the CAS Key Laboratory of Interfacial Physics and Technology (China); Supercomputer Center of Chinese Academy of Sciences and the Shanghai Supercomputer Center of China.

References

- [1] J.L. Herek, W. Wohlleben, R.J. Cogdell, D. Zeidler, and M. Motzkus, *Nature* **417**, 533 (2002). doi:10.1038/417533a.
- [2] G.S. Engel, T.R. Calhoun, E.L. Read, T.K. Ahn, T. Mančal, Y.C. Cheng, R.E. Blankenship, and G.R. Fleming, *Nature* **446**, 782 (2007). doi:10.1038/nature05678.
- [3] H. Lee, Y.C. Cheng, and G.R. Fleming, *Science* **316**, 1462 (2007). doi:10.1126/science.1142188.
- [4] M.R. Wasielewski, *Chem. Rev.* **92**, 435 (1992). doi:10.1021/cr00011a005.
- [5] D. Gust, T.A. Moore, and A.L. Moore, *Acc. Chem. Res.* **34**, 40 (2001). doi:10.1021/ar9801301.
- [6] D.M. Guldia, *Chem. Soc. Rev.* **31**, 22 (2002). doi:10.1039/b106962b.
- [7] M. Sarovar, A. Ishizaki, G.R. Fleming, and K.B. Whaley, *Nat. Phys.* **6**, 462 (2010). doi:10.1038/nphys1652.
- [8] N. Lambert, Y.N. Chen, Y.C. Cheng, C.M. Li, G.Y. Chen, and F. Nori, *Nat. Phys.* **9**, 10 (2013). doi:10.1038/nphys2474.
- [9] A. Ishizaki and G.R. Fleming, *Proc. Natl. Acad. Sci. U.S.A.* **106**, 17255 (2009). doi:10.1073/pnas.0908989106.
- [10] G. Panitchayangkoon, D. Hayes, K.A. Fransted, J.R. Caram, E. Harel, J. Wen, R.E. Blankenship, and G.S. Engel, *Proc. Natl. Acad. Sci. U.S.A.* **107**, 12766 (2010). doi:10.1073/pnas.1005484107.
- [11] A.A. Kerridge, *Phys. Chem. Chem. Phys.* **15**, 2197 (2013). doi:10.1039/c2cp43982d.
- [12] M. Gouterman, *J. Chem. Phys.* **30**, 1139 (1959). doi:10.1063/1.1730148.
- [13] J. Hasegawa, M. Hada, M. Nonoguchi, and H. Nakatsuji, *Chem. Phys. Lett.* **250**, 159 (1996). doi:10.1016/0009-2614(95)01406-3.
- [14] M. Rubio, B.O. Roos, L. Serrano-Andrés, and M. Merchán, *J. Chem. Phys.* **110**, 7202 (1999). doi:10.1063/1.478624.
- [15] E.J. Baerends, G. Ricciardi, A. Rosa, and S.J.A. van Gisbergen, *Coordin. Chem. Rev.* **230**, 5 (2002). doi:10.1016/S0010-8545(02)00093-0.
- [16] T. Hashimoto, Y.K. Choe, H. Nakano, and K. Hirao, *J. Phys. Chem. A* **103**, 1894 (1999). doi:10.1021/jp984807d.
- [17] J. Šeda, J.V. Burda, and J. Leszczynski, *J. Comput. Chem.* **26**, 294 (2005). doi:10.1002/jcc.20164.

- [18] J. Šeda, J.V. Burda, V. Brázdová, and V. Kapsa, *Int. J. Mol. Sci.* **5**, 196 (2004). doi:10.3390/i5040196.
- [19] V.G. Maslov, *Opt. Spectrosc.* **101**, 862 (2006). doi:10.1134/S0030400X06120071.
- [20] D. Sundholm, *Chem. Phys. Lett.* **317**, 392 (2000). doi:10.1016/S0009-2614(99)01422-0.
- [21] L. Edwards, D.H. Dolphin, and M. Gouterman, *J. Mol. Spectrosc.* **35**, 90 (1970). doi:10.1016/0022-2852(70)90168-2.
- [22] M. Fragata, B. Nordén, and T. Kurucsev, *Photochem. Photobiol.* **47**, 133 (1988). doi:10.1111/j.1751-1097.1988.tb02703.x.
- [23] M. Gouterman, in *The Porphyrins III*, edited by D. Dolphin (Academic Press, New York, NY, USA, 1978), pp. 1–165.
- [24] R. Schweitzer-Stenner and D. Bigman, *J. Phys. Chem. B* **105**, 7064 (2001). doi:10.1021/jp010703i.
- [25] A.A. Jarzqcki, P.M. Kozlowski, P. Pulay, B.H. Ye, and Y.X. Li, *Spectrochim. Acta A* **53**, 1195 (1997). doi:10.1016/S1386-1425(96)01870-7.
- [26] C.C. Díaz-Torrejón, F. Espinosa-Magaña, and I.G. Kaplan, *J. Mol. Struct. THEOCHEM* **955**, 39 (2010). doi:10.1016/j.theochem.2010.05.026.
- [27] M.P. Bucchino and L.M. Ziurys, *J. Phys. Chem. A* **117**, 9732 (2013). doi:10.1021/jp3123743.
- [28] M. Radoń, *J. Chem. Theory Comput.* **10**, 2306 (2014). doi:10.1021/ct500103h.
- [29] B. Song, M. Elstner, and G. Cuniberti, *Nano Lett.* **8**, 3217 (2008). doi:10.1021/nl801542g.
- [30] A. Heck, P.B. Woiczikowski, T. Kubař, K. Welke, T. Niehaus, B. Giese, S. Skourtis, M. Elstner, and T.B. Steinbrecher, *J. Phys. Chem. B* **118**, 4261 (2014). doi:10.1021/jp408907g.
- [31] T.J. Lee and H.F. Schaefer III, *J. Chem. Phys.* **83**, 1784 (1985). doi:10.1063/1.449367.
- [32] A.D. Becke, *J. Chem. Phys.* **98**, 5648 (1993). doi:10.1063/1.464913.
- [33] H.B. Schelegel, *J. Comp. Chem.* **3**, 214 (1982). doi:10.1002/jcc.540030212.
- [34] G.A. Peterssion and M.A. Al-Laham, *J. Chem. Phys.* **94**, 6081 (1991). doi:10.1063/1.460447.
- [35] M.S. Liao and S. Scheiner, *J. Chem. Phys.* **117**, 205 (2002). doi:10.1063/1.1480872.
- [36] J.R. Lakowicz, *Principles of Fluorescence Spectroscopy* (Springer, New York, 2006).
- [37] T. Otobe, M. Yamagiwa, J.-I. Iwata, K. Yabana, T. Nakatsukasa, and G.F. Bertsch, *Phys. Rev. B* **77**, 165104 (2008). doi:10.1103/PhysRevB.77.165104.
- [38] C. Wang, L. Jiang, F. Wang, X. Li, Y.P. Yuan, and H.L. Tsai, *Phys. Lett. A* **375**, 3200 (2011). doi:10.1016/j.physleta.2011.07.009.
- [39] G. García-Calderón and J. Villavicencio, *Phys. Rev. A* **68**, 052107 (2003). doi:10.1103/PhysRevA.68.052107.